

Integration of biocompatible organic resistive memory and photoresistor for wearable image sensing application

Qingyu CHEN¹, Min LIN¹, Yichen FANG¹, Zongwei WANG¹, Yuchao YANG^{1,2},
Jintong XU³, Yimao CAI^{1,2*} & Ru HUANG^{1,2}

¹*Institute of Microelectronics, Peking University, Beijing 100871, China;*

²*Research Center of Flexible Electronics, Peking University, Beijing 100871, China;*

³*Key Laboratory of Infrared Imaging Materials and Detectors, Shanghai Institute of Technical Physics, Chinese Academy of Sciences, Shanghai 200083, China*

Received 30 November 2017/Revised 3 January 2018/Accepted 10 January 2018/Published online 18 April 2018

Abstract The integration of multiple functional devices to achieve complex functions has become an essential requirement for future wearable biomedical electronic devices and systems. In this paper, we present a flexible multi-functional device composed of a biocompatible organic polymer resistive random-access memory (RRAM) and a photoresistor for wearable image sensing application. The resistive layer of organic polymer RRAM is composed by polychloro-para-xylylene (parylene-C), which is a flexible, transparent, biocompatibility and chemical stability polymer material. What is more, parylene-C is quite safe to be used within human body as it is a Food and Drug Administration (FDA)-approved material. This organic RRAM shows stable switching characteristics, low operation voltages (3.25 V for set voltage and -0.55 V for reset voltage), low static power consumption, high storage window and good retention properties ($>10^4$ s). A multi-functional device that can detect the light intensity of incident light and simultaneously store the information in the memory devices for wearable image sensing application was proposed and fabricated by integrating the organic resistive memory and a photoresistor. The threshold of incident light intensity can be easily adjust by changing the external voltage. This device is promising for building wearable electronic systems with various multiple functionalities.

Keywords wearable device, image sensor, flexible, biocompatible, resistive random-access memory (RRAM), photoresistor

Citation Chen Q Y, Lin M, Fang Y C, et al. Integration of biocompatible organic resistive memory and photoresistor for wearable image sensing application. *Sci China Inf Sci*, 2018, 61(6): 060411, <https://doi.org/10.1007/s11432-017-9356-4>

1 Introduction

In recent years, wearable biomedical electronic devices and systems have attract a lot of attention for their potential in modern medicine [1–3]. There are many types of electronic devices for wearable devices such as sensor, memory, transistor and battery [4–7]. And each device has its unique and irreplaceable function, but only one device is not enough for the biomedical electronic application, which usually need some more complex functions. As a result, it is necessary to integrate a biomedical electronic devices

* Corresponding author (email: caiyimao@pku.edu.cn)

system that contains many type of electronic devices on only one module [8–10]. Such a system can detect signal, process signal, store information and display the results only on an integrated system without any other help. What is more, safety is extremely important when these biomedical electronic devices and systems are implanted into the body, so the materials should be biocompatible to ensure these devices will not hurt the health of human.

Memory is an important component in the wearable biomedical electronic devices system to store the information detected by sensors. As an emerging non-volatile memory, resistive random-access memory (RRAM) has the advantages of low power consumption, simple structure, high switching speed and high intensity, and it is easy to integrate with other devices [11–18]. So RRAM is an appropriate memory for the wearable biomedical electronic devices and systems. Obviously, flexible memory is necessary for wearable electronics, but the traditional RRAM are made by metal oxide and they are all rigid and cannot work when the device is bent. In order to make the device flexible, 2D materials and organic polymer materials have often been used as active layer's material owing to their flexible structure [19–25]. Comparing with 2D materials, organic polymer materials are easier to fabricate and much cheaper, so organic RRAM is suitable for wearable devices and has been investigate widely. Polychloro-para-xylylene (parylene-C), as an organic polymer material, is quite flexible and transparent, which makes it becomes a suitable material for flexible RRAM. And parylene-C also has great chemical stability which ensure the parylene-C based RRAM can work stable in hard conditions. What is more, parylene-C is a Food and Drug Administration (FDA)-approved material, it means that parylene-C is a safe material to be used within human body.

Recently, the wearable image sensors have been widely investigated for their potential applications in machine vision systems and X-ray based biomedical imaging application [26–30]. As we know, an image sensor usually consists of a photosensitive element and a signal processing or storage element. Photoresistor, a light dependent resistor, exhibits obvious photoconductivity, which means that its resistance will decrease with increasing incident light intensity. So, photoresistor can be used as photosensitive element of image sensors. Nowadays, the signal processing or storage element of image sensors are mainly based on complementary metal-oxide-semiconductor (CMOS) or charge-coupled devices (CCD) [31–38]. However, both of them are difficult to be used in wearable and flexible devices due to their rigid Si-technology, so it is necessary to find a new device as wearable image sensor's signal processing or storage element. From the previous paragraph we can know, organic RRAM based on parylene-C is a suitable device for wearable and flexible devices. And, through the integration of photoresistor and RRAM, RRAM can direct store the signal detected by photoresistor. So, it is an adoptable method to integrate the parylene-C based RRAM and photoresistor as an image sensors system.

In this paper, we demonstrate a flexible multi-functional device composed of a biocompatible organic polymer resistive random-access memory and a photoresistor for image sensing application. The structure of our organic RRAM is Al/parylene-C/W on parylene-C substrate. Parylene-C is deposited by polymer chemical vapor deposition (CVD) at room temperature. Our device shows very good storage performance with stable switching characteristics, low switching voltage (3.25 V for set voltage and -0.55 V for reset voltage), remarkable storage window and good retention properties ($>10^4$ s). The high resistance of our RRAM is quite high (>10 M Ω), resulting in an extremely low static power consumption. What is more, parylene-C is quite flexible and biocompatible, implying that this device is a suitable device to be integrated into the wearable biomedical electronic devices and systems. Then, we integrate our organic resistive memory with a photoresistor to fabricate a multi-functional device. When the multi-functional device is illuminated by an external light source, the RRAM will switch to low resistance state if the incident light intensity exceed the threshold. It means that the information of the incident light intensity can be direct stored in RRAM. Besides, we can easily adjust the threshold of incident light intensity by changing the external voltage applied on the device. The device also can be easily read and erased. These results are valuable for the integrated of multiple devices into a single module and also provide new opportunities for future biomedical electronic devices and systems.

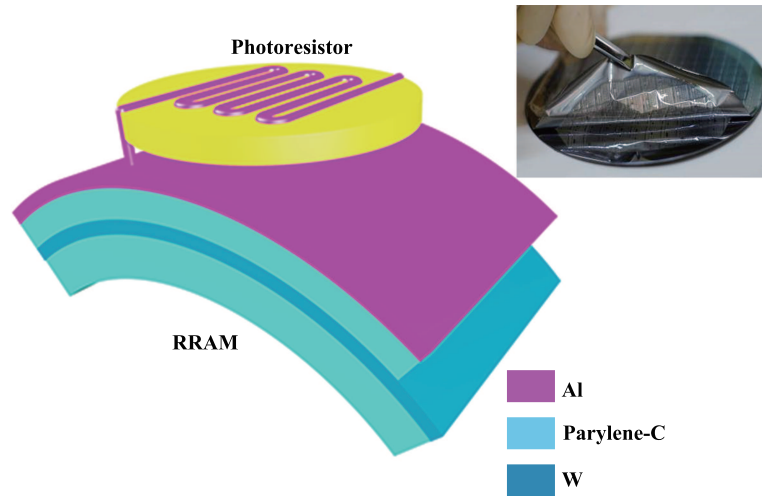


Figure 1 (Color online) The schematic of our flexible multi-functional device which integrates a parylene-C based resistive memory and a photoresistor. The illustration in the upper right indicates that our flexible organic RRAM can be easily torn off the silicon wafer.

2 Materials and methods

Figure 1 shows a schematic image of the multi-functional device, which consists of a flexible resistive memory and a photoresistor. The structure of our organic polymer RRAM, which is fabricated on parylene-C substrate, is Al/parylene-C/W. And the fabrication process of RRAM are as follows. At first, parylene-C substrate with a thickness of 5 μm was deposited on the silicon wafer with polymer CVD at room temperature by using specialty coating systems PDS2010. Then, 200 nm tungsten (W) was sputtered upon parylene-C substrate and followed by a lift-off process as bottom electrodes (BE). After that, parylene-C with a thickness of 40 nm was deposited by polymer CVD as active layer at room temperature. Then, the BE via were pattern by lithography and reactive ion etching. Finally, 200 nm aluminum (Al) was sputtered upon it and followed by a lift-off process as top electrodes (TE). Figure 2 shows the schematic of the polymer CVD process of the parylene-C thin film. The special coating systems PDS2010 mainly consists of the vaporizer part, the pyrolysis zone and the deposition chamber. At first, the solid dimer is heated and slowly vaporizes at about 175 $^{\circ}\text{C}$ in the vaporizer part. Then, the dimer gas will be cleaved into the monomer gas when it flows into the pyrolysis part, which is about 690 $^{\circ}\text{C}$. Finally, the monomer will polymerize in the deposition chamber at room temperature. It is worth noting that our device can be removed from the wafer directly without any other process, as shown in the illustration in the upper right of Figure 1. And the size of the device is 5 μm \times 5 μm in our experiment.

Then, we integrate our flexible parylene-C based RRAM with the photoresistor to fabricate the multi-functional device, as shown in Figure 1. It is worth mentioning that there is a fixed value resistor ($R_{//}$) in parallel with the RRAM in this experiment. An external voltage (V_{total}) is applied on the multi-functional device when it works in writing mode. The resistance of this fixed value resistor is 110 k Ω , which is between the bright resistance (>5 k Ω) and the dark resistance (\sim 1 G Ω) of photoresistor. The function of the parallel fixed value resistor is to ensure the change of resistance of photoresistor can effectively influence the voltage applied on the RRAM. And when this multi-functional device works in reading mode or erasing mode, the voltages are applied on the RRAM directly. The integration of RRAM and photoresistor enable them to achieve complex functions.

All of the electrical characteristics of our devices were measured by Agilent B1500A (Keysight Technologies, Santa Rosa, California, CA, USA) in an ambient air environment. During the measurements of RRAM, the top Al electrode was applied with a voltage bias and the bottom W electrode was grounded. What is more, a compliance current was set to 1 mA to avoid a hard dielectric breakdown in the set process. Parylene-C was purchased from SCS, Indianapolis, Indiana, IN, USA, and the photoresistor (GM

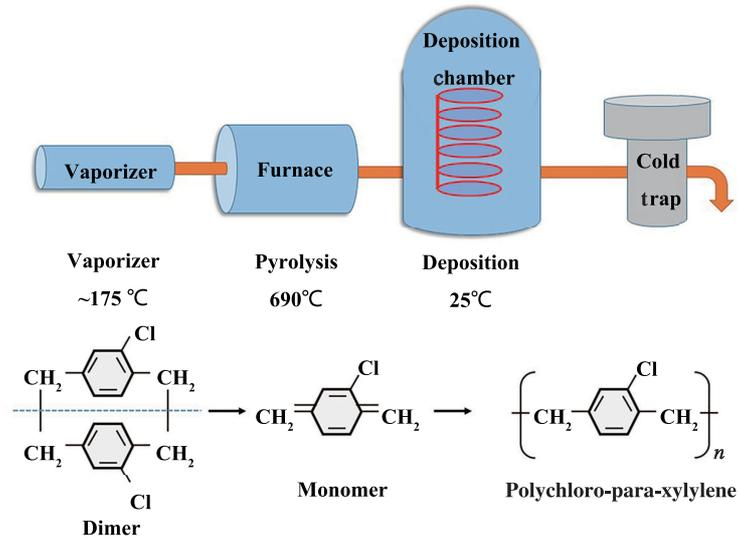


Figure 2 (Color online) The schematic of the polymer CVD process of the parylene-C thin film.

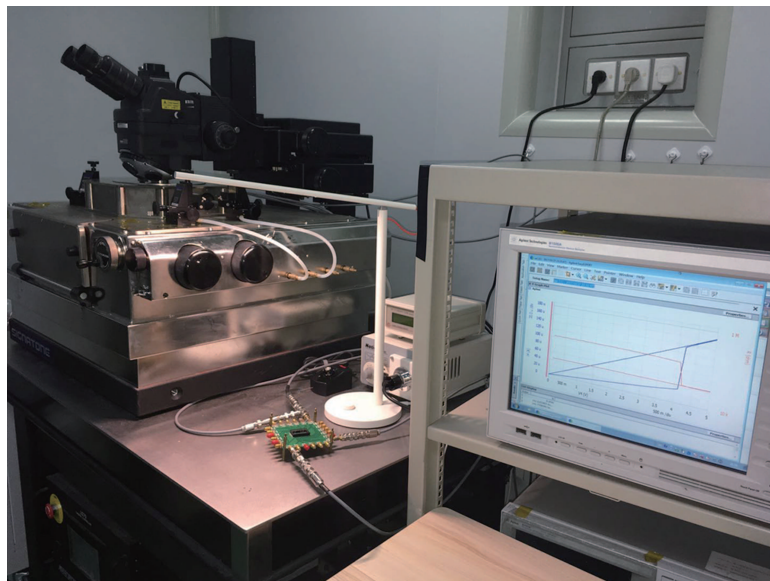


Figure 3 (Color online) The test system in this experiment.

5549) were purchased for TaoTimeClub, Shenzhen, China. The incident light is the visible light, and it was provided by a commercial lamp which can adjust the brightness slightly. And the light intensity is expressed as the brightness percentage of lamp in this paper. The test system in this experiment is shown in Figure 3.

3 Discussion and conclusion

3.1 Resistive switching characteristics

Figure 4 shows the typical switching characteristics of our Al/parylene-C/W device. Initially, the resistance state of our devices are in high resistance state (HRS), and it is worth mentioning that our devices are all forming-free. And the device shows a bipolar resistance characteristics. So, when the voltage applied upon top electrode is larger than the set voltage ($V_{\text{set}}=3.25 \text{ V}$), the resistance will switch from

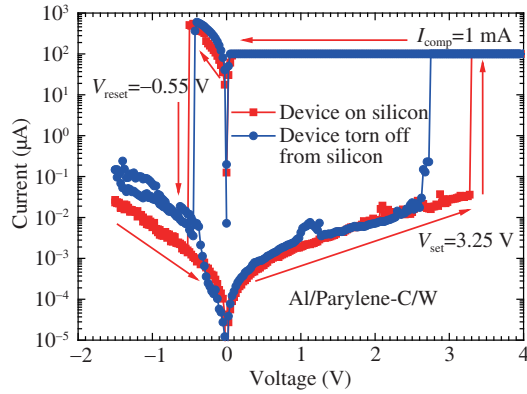


Figure 4 (Color online) (Red) Measured typical I-V curve of our Al/parylene-C/W device. Arrows show the voltage sweep direction and the extracted set and reset voltage are 3.25 V and -0.55 V, respectively. The resistance window is quite high, and the set compliance current is 1 mA. (Blue) Typical I-V curve after the bended device was torn off from the silicon wafer.

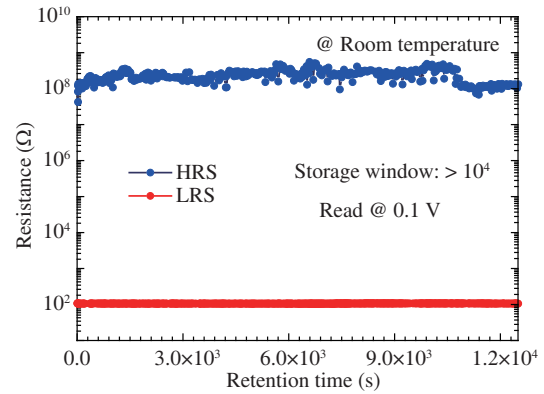


Figure 5 (Color online) The retention behavior of our parylene-C based device measured by applying a 0.1 V read voltage at room temperature. There is no apparent degradation after 10^4 s for both LRS and HRS.

high resistance state to low resistance state (LRS) abruptly. Then, it will switch back to high resistance state abruptly when the applied voltage is lower than the reset voltage ($V_{\text{reset}} = -0.55$ V). The set voltage and reset voltage are both low and hence suitable for the low power wearable devices application. In addition, a high resistance window has been achieved, and the high resistance is higher than 10 M Ω . As a result, the static power consumption is extremely low ($<10^{-4}$ mW @ 1 V), which are quite valuable for low power wearable devices. The typical switching characteristics of the bended device which was torn off from the silicon wafer has also been shown in the blue curve of Figure 4. It is worth noting that the bended device also shows good storage performance, indicating the potential for the wearable device. The retention characteristic of our device has also been measured at room temperature, as shown in Figure 5. There is no apparent degradation for both high resistance state and low resistance state after 10^4 s, which means a good retention properties for organic resistive memory. These results indicate that our devices are a nice choice for wearable devices.

3.2 Multi-functional device for image sensing application

The information storage and light sensing functions have been carried out on our multi-functional device. At first, the typical I-V curve of the multi-functional device at bright environment has been measured to prove that the RRAM can work normally when it is integrated with a photoresistor, as shown in Figure 6. Here, the bright resistance of photoresistor (R_{Bright}) is about 30 k Ω , so the total resistance of the device is about 140 k Ω ($\approx R_{\text{Bright}} + R_{//}$) before RRAM is switched to low resistance state. Then, when the external voltage applied on the device is large enough, the total resistance of the device will be reduced to about 30 k Ω , which is equal to the bright resistance of photoresistor approximately. It is because that the voltage applied on RRAM device will get larger than its set voltage as the external voltage increases, as a result, the RRAM will be switched to low resistance state. After RRAM is switched to low resistance state, the total resistance will approximate equal to the bright resistance of the photoresistor because the low resistance of RRAM is much lower than that of photoresistor, as shown in the red line of Figure 6. These results indicate that the RRAM can work normally when we integrate it with a photoresistor.

Figure 7 shows the writing process of our multi-functional device. Initially, the multi-functional device is in a dark environment ($R_{\text{Dark}} \approx 1$ G Ω) and the RRAM is in its high resistance state. An external voltage is applied on this device, but the voltage will mainly drops on the photoresistor because the dark resistance of photoresistor (≈ 1 G Ω) is much larger than the parallel resistance of RRAM and fixed value resistor (≈ 110 k Ω). Then, when the light is on at about 10 s, the resistance of photoresistor will

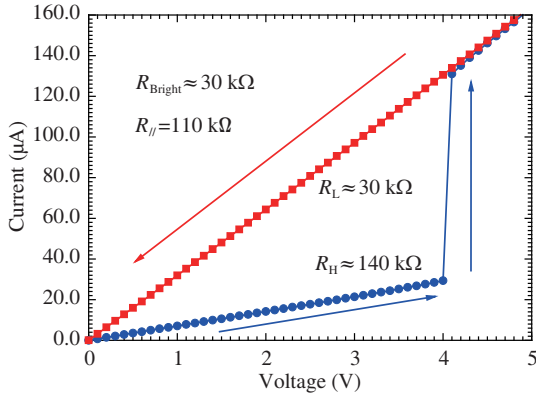


Figure 6 (Color online) The typical I-V curve of the writing process of our multi-functional device at bright environment.

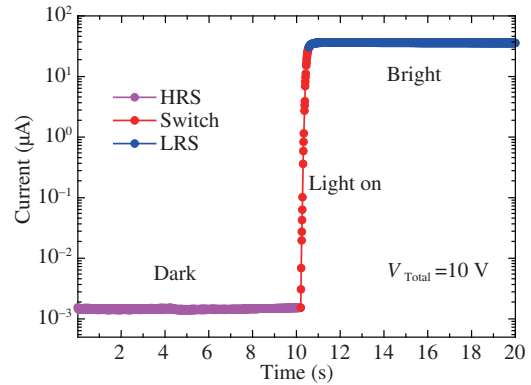


Figure 7 (Color online) The writing process of our multi-functional device. At about 10 s, the light is on, which resulted in the switching of RRAM.

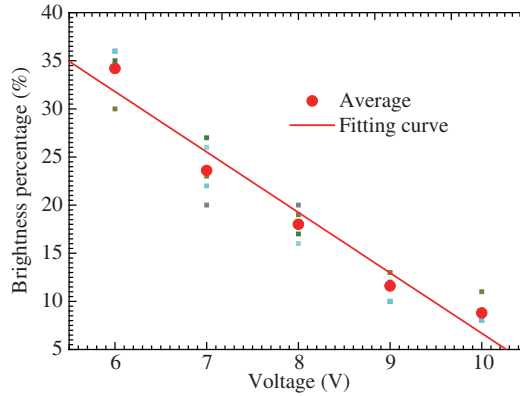


Figure 8 (Color online) The relationship between the total voltages applied on the multi-functional device and the threshold of light intensity of the incident light that just can switch the RRAM. Here, the light intensity of the incident light is expressed as the brightness percentage of the lamp. The threshold of light intensity will decrease when the total voltages increase.

drops down to approximately 30 kΩ immediately. As a result, most of the voltage will drop on RRAM, indicating that RRAM will be switched to low resistance state. As a result, the information of incident light has been stored in RRAM successfully. What is more, if we want to erase the information stored in RRAM, we can directly apply a negative reset voltage on RRAM. And the reading operation is similar to the erasing process. The above results show that the incident light can be sensed by our multi-functional device when its light intensity exceeded the threshold, and the information of incident light can be directly stored in RRAM simultaneously.

It will be useful to enable the device to modify the sensing threshold of light intensity in real application. Measurement shows that the threshold of light intensity to switch the RRAM is dependent on the given external voltage. In measurement we investigate the relationship between the total voltages applied on the multi-functional device and the threshold of light intensity of the incident light, the results are shown in Figure 8. Here, the light intensity of the incident light is expressed as the brightness percentage of the lamp. From Figure 8 we can know, the threshold of light intensity of the incident light will decrease if the external voltage applied on the device increases. This is because that the RRAM is in series with the photoresistor, as shown in Figure 1. So the percentage of the separate voltage applied on RRAM will increase when the incident light becomes brighter, which causes the reduction of the resistance of photoresistor. As a result, the RRAM will be switched to low resistance state if its separate voltage is larger than its set voltage. For the RRAM which has a larger external voltage, it just needs a smaller percentage of separate voltage on RRAM to reach its set voltage. So, the threshold of light intensity of

the incident light will decrease when the external voltage applied on the multi-functional device become larger. In other words, there is a unique threshold of light intensity for a given external voltage, and we can easily adjust the threshold of incident light intensity by changing the external voltage applied on the device.

3.3 Conclusion

In summary, we have successfully fabricated a flexible multi-functional device integrated with a biocompatible parylene-C based RRAM and a photoresistor for image sensing application. Our organic RRAM shows quite superb storage property and the retention characteristic of RRAM is also good enough for wearable devices. What is more, it shows great biocompatibility, which make it harmless to human body and becomes a quite suitable device for biomedical electronic device. After integrated with photoresistor, the RRAM can also be written and read normally. The multi-functional device can detect the light intensity of incident light and simultaneously store the information in the memory devices for wearable image sensing application. Besides, the threshold of incident light intensity can be adjust by changing the external voltage applied on the multi-functional device. This device is promising for application of wearable biomedical electronic systems with multi-functions.

Acknowledgements This work was supported in part by National Natural Science Foundation of China (Grant Nos. 61574007, 61376087, 61421005), Beijing Municipal Science and Technology Commission Program (Grant No. Z16110000216148), and Key Laboratory of Infrared Imaging Materials and Detectors, Shanghai Institute of Technical Physics, Chinese Academy of Sciences (Grant No. IIMDKFJJ-14-08).

References

- 1 Choi S, Lee H, Ghaffari R, et al. Recent advances in flexible and stretchable bio-electronic devices integrated with nanomaterials. *Adv Mater*, 2016, 28: 4203–4218
- 2 Gao W, Emaminejad S, Nyein H Y Y, et al. Fully integrated wearable sensor arrays for multiplexed in situ perspiration analysis. *Nature*, 2016, 529: 509–514
- 3 Pang C, Lee C, Suh K Y. Recent advances in flexible sensors for wearable and implantable devices. *J Appl Polym Sci*, 2013, 130: 1429–1441
- 4 Shao Y Y, Wang J, Wu H, et al. Graphene based electrochemical sensors and biosensors: a review. *Electroanalysis*, 2010, 22: 1027–1036
- 5 Kim S, Jeong H Y, Kim S K, et al. Flexible memristive memory array on plastic substrates. *Nano Lett*, 2011, 11: 5438–5442
- 6 Kim J, Lee M S, Jeon S, et al. Highly transparent and stretchable field-effect transistor sensors using graphene-nanowire hybrid nanostructures. *Adv Mater*, 2015, 27: 3292–3297
- 7 Wang X F, Lu X H, Liu B, et al. Flexible energy-storage devices: design consideration and recent progress. *Adv Mater*, 2014, 26: 4763–4782
- 8 Trung T Q, Lee N E. Flexible and stretchable physical sensor integrated platforms for wearable human-activity monitoring and personal healthcare. *Adv Mater*, 2016, 28: 4338–4372
- 9 Lee H, Choi T K, Lee Y B, et al. A graphene-based electrochemical device with thermoresponsive microneedles for diabetes monitoring and therapy. *Nat Nanotech*, 2016, 11: 566–572
- 10 Son D, Lee J, Qiao S T, et al. Multifunctional wearable devices for diagnosis and therapy of movement disorders. *Nat Nano*, 2014, 9: 397–404
- 11 Pan F, Gao S, Chen C, et al. Recent progress in resistive random access memories: materials, switching mechanisms, and performance. *Mater Sci Eng R Rep*, 2014, 83: 1–59
- 12 Wong H S P, Lee H Y, Yu S M, et al. Metal-oxide RRAM. *Proc IEEE*, 2012, 100: 1951–1970
- 13 Liu Q, Sun J, Lv H B, et al. Real-time observation on dynamic growth/dissolution of conductive filaments in oxide-electrolyte-based ReRAM. *Adv Mater*, 2012, 24: 1844–1849
- 14 Yang Y C, Gao P, Gaba S, et al. Observation of conducting filament growth in nanoscale resistive memories. *Nat Commun*, 2012, 3: 732
- 15 Yu M X, Cai Y M, Wang Z W, et al. Novel vertical 3D structure of TaO_x-based RRAM with self-localized switching region by sidewall electrode oxidation. *Sci Rep*, 2016, 6: 21020
- 16 Cheng C H, Yeh F S, Chin A. Low-power high-performance non-volatile memory on a flexible substrate with excellent endurance. *Adv Mater*, 2011, 23: 902–905
- 17 Long S B, Liu Q, Lv H B, et al. Research progresses of resistive random access memory (in Chinese). *Sci Sin-Phys Mech Astron*, 2016, 46: 107311

- 18 Hudec B, Hsu C W, Wang I T, et al. 3D resistive RAM cell design for high-density storage class memory—a review. *Sci China Inf Sci*, 2016, 59: 061403
- 19 Shin G H, Kim C K, Bang G S, et al. Multilevel resistive switching nonvolatile memory based on MoS₂ nanosheet-embedded graphene oxide. *2D Mater*, 2016, 3: 034002
- 20 Puglisi F M, Larcher L, Pan C, et al. 2D h-BN based RRAM devices. In: Proceedings IEEE International Electron Devices Meeting (IEDM), San Francisco, 2016
- 21 Casula G, Cosseddu P, Bonfiglio A. Integration of an organic resistive memory with a pressure-sensitive element on a fully flexible substrate. *Adv Electron Mater*, 2015, 1: 1500234
- 22 Son D, Chae S I, Kim M, et al. Colloidal synthesis of uniform-sized molybdenum disulfide nanosheets for wafer-scale flexible nonvolatile memory. *Adv Mater*, 2016, 28: 9326–9332
- 23 Choi J, Park S, Lee J, et al. Organolead halide perovskites for low operating voltage multilevel resistive switching. *Adv Mater*, 2016, 28: 6562–6567
- 24 Wang C Y, Gu P Y, Hu B L, et al. Recent progress in organic resistance memory with small molecules and inorganic-organic hybrid polymers as active elements. *J Mater Chem C*, 2015, 3: 10055–10065
- 25 Liu G, Zhuang X D, Chen Y, et al. Bistable electrical switching and electronic memory effect in a solution-processable graphene oxide-donor polymer complex. *Appl Phys Lett*, 2009, 95: 253301
- 26 Nau S, Wolf C, Sax S, et al. Organic non-volatile resistive photo-switches for flexible image detector arrays. *Adv Mater*, 2015, 27: 1048–1052
- 27 Pierre A, Gaikwad A, Arias A C. Charge-integrating organic heterojunction phototransistors for wide-dynamic-range image sensors. *Nat Photon*, 2017, 11: 193–199
- 28 Yakunin S, Sytnyk M, Kriegner D, et al. Detection of X-ray photons by solution-processed lead halide perovskites. *Nat Photon*, 2015, 9: 444–449
- 29 Tian L, Luo X L, Yin M, et al. Enhanced CMOS image sensor by flexible 3D nanocone anti-reflection film. *Sci Bull*, 2017, 62: 130–135
- 30 Zhao Q, Huang C H, Li F Y. Phosphorescent heavy-metal complexes for bioimaging. *Chem Soc Rev*, 2011, 40: 2508–2524
- 31 Fossum E R, Hondongwa D B. A review of the pinned photodiode for CCD and CMOS image sensors. *IEEE J Electron Devices Soc*, 2014, 2: 33–43
- 32 Goossens S, Navickaite G, Monasterio C, et al. Broadband image sensor array based on graphene-CMOS integration. *Nat Photon*, 2017, 11: 366–371
- 33 Theuwissen A J P. CMOS image sensors: state-of-the-art. *Solid State Electron*, 2008, 52: 1401–1406
- 34 Huang W, Xu Z Y. Characteristics and performance of image sensor communication. *IEEE Photon J*, 2017, 9: 7902919
- 35 El-Desouki M, Deen M J, Fang Q Y, et al. CMOS image sensors for high speed applications. *Sensors*, 2009, 9: 430–444
- 36 Shin B, Park S, Shin H. The effect of photodiode shape on charge transfer in CMOS image sensors. *Solid-State Electron*, 2010, 54: 1416–1420
- 37 Zhou Y F, Cao Z X, Han Y, et al. A low power global shutter pixel with extended FD voltage swing range for large format high speed CMOS image sensor. *Sci China Inf Sci*, 2015, 58: 042406
- 38 Xue Y Y, Wang Z J, Liu M B, et al. Research on proton radiation effects on CMOS image sensors with experimental and particle transport simulation methods. *Sci China Inf Sci*, 2017, 60: 120402